Computer Communications xxx (2010) xxx–xxx

Contents lists available at ScienceDirect

Computer Communications

journal homepage: www.elsevier.com/locate/comcom

On a moving direction pattern based MAP selection model for HMIPv6 networks

Jinsuk Baek [a], Jan Fischer [b], Hsiao-Hwa Chen [c,*], Minho Jo [d,**]

[a] Department of Computer Science, Winston-Salem State University, USA
[b] Department of Computer Science, Universitat Karlsruhe, Germany
[c] Department of Engineering Science, National Cheng Kung University, 1 Da-Hsueh Road, Tainan City 70101, Taiwan
[d] School of Electrical Engineering, Korea University, 5-ka, Anam-dong, Seongbuk-Gu, Seoul 136-701, South Korea

ARTICLE INFO

Article history:
Available online xxxx

Keywords:
MAP selection
HMIPv6 network
Binding update cost
Packet delivery cost
Load balance

ABSTRACT

In a large-scale mobile IPv6 network, usually there are several coexisting mobility anchor points (MAPs) for networking robustness and traffic sharing. Therefore, it is a challenging issue for an arriving mobile node to choose the most appropriate MAP to bind. This task must be carried out by considering the issues of load balancing, binding update and packet delivery cost minimization. This paper proposes a novel MAP selection scheme for hierarchical mobile IPv6 networks to allow a mobile node to discover the most appropriate MAP when there are multiple coexisting MAPs. This scheme is an enhancement to the adaptive MAP selection scheme. The proposed scheme improve the overall performance due to the consideration of the movement (direction) pattern of mobile nodes. Simulation results show that this scheme outperforms the existing cost models in terms of total binding update and packet delivery costs, ensuring a level of load balance similar to adaptive MAP selection scheme.

1. Introduction

Mobile communication has become an indispensable part of our daily life due to the widespread use of portable computers and handheld devices, such as PDAs and smart phones, etc. While roaming between different IP networks, mobile users access the Internet to retrieve emails and other information, and communicate with people via video conferencing. Recently, a growing number of mobile applications require mobile users to transmit multimedia data in wireless environments at a relatively high transmission rate.

In order to transmit time-sensitive or real-time multimedia data in a mobile wireless environment, seamless handoff must be provided. In order to facilitate mobile roaming between different wireless or wired access networks, various mobile IP (MIP) protocols were introduced by the Internet Engineering Task Force (IETF). In the mobile IPv4 (MIPv4) protocol [1–4], registration can be done in some specialized routers such as foreign agents (FAs) or home agents (HAs). On the other hand, mobile IPv6 (MIPv6) [5] does not require dedicated routers to act as FAs. Both protocols allow a mobile node (MN) to maintain a permanent IP address (viz., the home address) while visiting different networks. The HA redirects packets to the MN while the MN is away from its home network. Whenever an MN changes its point of attachment, both protocols require the MN to update its HA with its new location and all correspondent nodes (CNs) communicating with the MN. Even if the MN roams between subnets within the same domain, the MN must send a binding update (BU) to the HA, which usually resides far from the location of the MN.

To reduce the signaling overhead caused by the handover process, the concept of mobility anchor point (MAP) was introduced in the hierarchical MIPv6 (HMIPv6) protocol [6] and its functionality was extended in many follow-up studies [7,8]. An MAP serves as a local HA in a foreign network. Whenever an MN moves to a new subnet within the same domain, it sends a BU to the MAP, rather than the HA. This reduces the signaling overhead significantly, since the MAP is usually much closer to the MN than the HA. Within a large-scale network infrastructure, there are usually several coexisting MAPs to improve robustness and enable traffic sharing. As a result, in a given MAP domain, an arriving MN has the task of determining and binding to the most appropriate MAP. When the MN must select the proper MAP in a given domain, selection stability, load balancing among MAPs, BU and packet delivery (PD) costs are important criteria for achieving the optimal performance.

While acknowledging the previous schemes [11–19] which were found to be efficient, we need to point out that they only focused on one or two influencing factors for determining the most suitable MAP. As a result, many previous schemes work effectively only in some specific cases. However, in general, there might exist some more suitable MAPs than those proposed by the aforementioned MAP selection procedures.

The contributions of this paper are summarized as follows. We propose an improved MAP selection scheme, which is an

* Corresponding author. Tel.: +886 6 2757575x63320; fax: +886 6 2766549.
** Corresponding author. Tel.: +82 2 3290 4764; fax: +82 2 928 9109.
E-mail addresses: baekj@wssu.edu (J. Baek), jan-fi@gmx.de (J. Fischer), hshwchen@ieee.org (H.-H. Chen), minhojo@korea.ac.kr, minhojo@gmail.com (M. Jo).

0140-3664/$ - see front matter © 2010 Elsevier B.V. All rights reserved.
doi:10.1016/j.comcom.2010.03.030

enhancement to the most recently reported scheme reported in [15]. The proposed scheme can discover a better MAP in terms of total BU and PD costs, while still maintaining the MAP load balance and outperforming the existing schemes. Compared with the existing methods, the proposed scheme takes into account almost all important factors which have impact on the MAP selection process, including (1) the handoff frequency of an MN; (2) the direction of movement of an MN; (3) the expected BU costs (depending on the selected MAP); and (4) the expected packet delivery costs (depending on the selected MAP). In particular, we consider the movement patterns of an MN in this paper. These considerations affect the processing load of an MAP and selection stability.

The remainder of this paper is outlined as follows. Section 2 discusses the related works and the problems with existing MAP selection schemes. Section 3 proposes our MAP selection scheme as an effort to improve the existing schemes. In Section 4, we investigate the proposed scheme via analysis and show the performance of the proposed scheme, followed by the conclusions and future works given in Section 5.

2. Existing works

Several MAP selection schemes were proposed in the literature. The furthest MAP selection (FMS) scheme [16] selects the furthest MAP along the transmission route from the MN to the HA. This scheme works based on the assumption that an MAP residing far from the MN is most likely to be reachable eventually. As a consequence, resource-consuming BU messages to the HA and correspondent nodes (CNs) are avoided because the MN's care-of-address (CoA) remains unmodified. However, the furthermost MAP is likely the gateway of a foreign network. Consequently, all MNs may select the gateway as their most appropriate MAP as it represents the MAP furthest away from all MNs. This results in possible overloading of the gateway node, leading to congestion and a single point of failure. Moreover, the scheme assumed that every MN has a wide mobility range and therefore needs to register at an MAP with the largest domain. However, many MNs may have only relatively small mobility ranges such as the MNs residing in offices. In this case, selecting a closer MAP is enough to reduce registration delays.

The multilevel hierarchically distributed IP mobility management (MHDS) scheme [13] selects the most appropriate MAP based on the MN's speed. The velocity-based scheme distinguishes MAPs with wider domains (higher MAPs) from MAPs with narrower domains (lower MAPs). Then, it assigns lower MAPs to lower speed MNs and higher MAPs to higher speed MNs within the network. The velocity-based scheme reduces the average number of BUs to the HA as well as the average number of managed MNs using an MAP. However, the other important factors such as expected PD costs during one session and movement direction patterns of the MNs were not considered.

Yet another scheme is the adaptive MAP selection (AMS) scheme [15], which forms the basis for the MAP selection scheme, or advanced AMS (AAMS) proposed in this paper. First, it estimates a special parameter, viz., session-to-mobility ratio (SMR), which is based on the number of handoffs and session arrivals in which an MN is involved. This parameter is used to determine when a new MAP selection process must be initiated. The total cost for each available MAP is calculated via the sum of expected BU and PD costs and then it selects the MAP with the lowest total cost. Although the AMS scheme considers BU and PD costs jointly, it does not consider the MN's direction of movement, which is an important parameter in MAP selection.

In addition to the aforementioned schemes, various improved schemes [5,11,12] were also proposed. Unfortunately, these schemes focused on a limited number of factors determining the MAP. Also, some other schemes [9,10] which intend to reduce handover latency for different target networks such as wireless mesh network (WMN) have been proposed. In the section followed, our scheme is introduced as an effort to improve the performance of all aforementioned schemes.

3. Proposed map selection scheme

The proposed MAP selection scheme works in four phases during the entire MAP selection procedure, including: (1) Initialization, (2) MAP evaluation, (3) MAP selection, and (4) MAP revision. The procedure is shown in Fig. 1. This section explains each of the four phases. A detailed description is provided in the corresponding subsections. The Initialization phase starts whenever an MN enters a new MAP domain. Arriving at a foreign network, the MN starts retrieving router advertisement (RA) messages. By collecting RA messages, the MN obtains important information about all available MAPs in the domain, such as hop distances, etc. The MAP evaluation follows the initialization immediately. The MN evaluates all available MAPs via information obtained in the previous procedure. In this scheme, we take into account the parameters of BU and PD costs. In the MAP selection phase, the MN is bound to the most suitable MAP. The decision is made based on the results of the MAP evaluation procedure. After the MN is bound to the most suitable MAP, it must determine whether or not the chosen MAP is still the most suitable one. This task is handled periodically in the MAP revision phase.

3.1. Initialization

An MN starts the initialization process immediately after the MAP revision phase detects that the MN's current MAP is not the

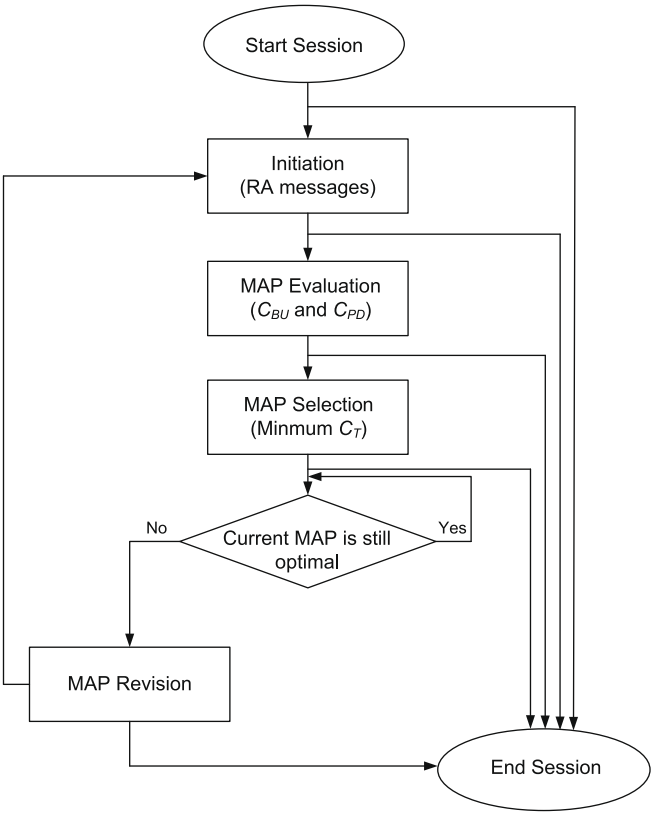

Fig. 1. Flow chart for the proposed MAP selection scheme.

Please cite this article in press as: J. Baek et al., On a moving direction pattern based MAP selection model for HMIPv6 networks, Comput. Commun. (2010), doi:10.1016/j.comcom.2010.03.030

most suitable one or no longer available. This is basically the case when an MN enters a new MAP domain. During a predefined time period, viz., a search interval, the MN collects RA messages sent by access routers (ARs) within the range. Each RA message contains a list of available MAPs as well as their hop distances to the MN. The MN stores this information in a data structure or an MAP list. The MAP list contains pairs of MAP IP addresses and hop distances for each MAP, and is included in the RA message. After storing the data, the MN initiates the MAP evaluation.

3.2. MAP evaluation

3.2.1. BU cost function model

In the original BU cost function model [15], the expected BU costs resulting from binding to one MAP are calculated. There are two types of BUs, namely BU-to-MN-HA and BU-to-MN-MAP. By defining N_C as the number of subnet crossings in an MAP domain per session and N_D as the number of MAP domain crossings per session, the BU costs per session are expressed by

$$C_{BU} = E(N_C)U_{MAP} + E(N_D)U_{HA}, \tag{1}$$

where U_{MAP} and U_{HA} are the BU costs to the MN's MAP and HA, respectively.

Assume that U_{HA} is known and U_{MAP} can be obtained by RA messages during the initialization phase in terms of the hop distance. The accuracy of (1) is dependent only on the precision of estimation of $E(N_C)$ and $E(N_D)$, the average number of subnet, and MAP domain crossings per session. In order to calculate $E(N_C)$ and $E(N_D)$, the subnet crossing probability P_C and MAP domain crossing probability P_D are expressed for each session, based on the inter-session time t_S, subnet residence time t_C, and MAP domain residence time t_D, which can be expressed as follows:

$$P_C = P(t_S > t_C), \tag{2}$$

$$P_D = P(t_S > t_D). \tag{3}$$

The probability density functions of N_C and N_D are deduced from Eqs. (2) and (3). Eqs. (4) and (5) express the likelihood that an MN crosses n subnets per session and an MN crosses n MAP domains within a session, respectively.

$$P(N_C = n) = P_C^n(1 - P_C), \tag{4}$$

$$P(N_D = n) = P_D^n(1 - P_D). \tag{5}$$

Then, $E(N_C)$ and $E(N_D)$ are expressed by

$$P(N_C) = \sum_{n=0}^{\infty} nP_C^n(1 - P_C), \tag{6}$$

$$P(N_D) = \sum_{n=0}^{\infty} nP_D^n(1 - P_D). \tag{7}$$

Because of its memoryless property, an exponential distribution is used to describe t_S, t_C, and t_D with their rates being λ_S, μ_C, and μ_D, respectively. Then, P_C and P_D are calculated by

$$\begin{aligned} P_C = P(t_S > t_C) &= \int_0^{\infty} P(t_S > \tau)\mu_C e^{-\mu_C \tau}\, d\tau \\ &= \int_0^{\infty} \left(\int_{\tau}^{\infty} \lambda_S e^{\lambda_S \sigma}\, d\sigma \right) \mu_C e^{-\mu_C \tau}\, d\tau \\ &= \int_0^{\infty} [-e^{-\lambda_S \tau}]_0^{\infty} \mu_C e^{-\mu_C \tau}\, d\tau = \int_0^{\infty} e^{-\lambda_S \tau} \mu_C e^{-\mu_C \tau} \\ &= \frac{\mu_C}{\mu_C + \lambda_S}, \end{aligned} \tag{8}$$

$$\begin{aligned} P_D = P(t_S > t_D) &= \int_0^{\infty} P(t_S > \tau)\mu_D e^{-\mu_D \tau}\, d\tau = \int_0^{\infty} e^{-\lambda_S \tau} \mu_D e^{-\mu_D \tau} \\ &= \frac{\mu_D}{\mu_D + \lambda_S}. \end{aligned} \tag{9}$$

By substituting Eqs. (8) and (9) into Eqs. (6) and (7), respectively, the expectation of the number of subnet and MAP crossings is given by

$$\begin{aligned} E(N_C) &= \sum_{n=0}^{\infty} n \left(\frac{\mu_C}{\mu_C + \lambda_S} \right)^n \left(1 - \frac{\mu_C}{\mu_C + \lambda_S} \right) \\ &= \left(1 - \frac{\mu_C}{\mu_C + \lambda_S} \right) \frac{\frac{\mu_C}{\mu_C + \lambda_S}}{\left(1 - \frac{\mu_C}{\mu_C + \lambda_S} \right)^2} = \frac{\mu_C}{\lambda_S}, \end{aligned} \tag{10}$$

$$\begin{aligned} E(N_D) &= \sum_{n=0}^{\infty} n \left(\frac{\mu_D}{\mu_D + \lambda_S} \right)^n \left(1 - \frac{\mu_D}{\mu_D + \lambda_S} \right) \\ &= \left(1 - \frac{\mu_D}{\mu_D + \lambda_S} \right) \frac{\frac{\mu_D}{\mu_D + \lambda_S}}{\left(1 - \frac{\mu_D}{\mu_D + \lambda_S} \right)^2} = \frac{\mu_D}{\lambda_S}. \end{aligned} \tag{11}$$

Finally, the BU costs per session given by Eq. (1) can be expressed by

$$C_{BU} = \frac{\mu_C}{\lambda_S} U_{MAP} + \frac{\mu_D}{\lambda_S} U_{HA}. \tag{12}$$

To simplify Eq. (12), the subnet crossing rate μ_C is expressed in terms of the MAP domain crossing rate μ_D. The domain crossing rate is proportional to the subnet crossing rate and inversely proportional to the number of subnets in an MAP domain. Let n be the number of subnets and k_1 be a proportional coefficient ($k_1 \geqslant 0$). Then the domain crossing rate μ_D can be approximated by $\mu_C/\sqrt{n/k_1}$, from which the BU cost function can be simplified into

$$C_{BU} = \frac{\mu_D}{\lambda_S} \left(\sqrt{\frac{n}{k_1}} U_{MAP} + U_{HA} \right). \tag{13}$$

The accuracy of Eq. (13) depends only on the estimation of λ_S and μ_D, as U_{HA} and U_{MAP} are given by the obtained router advertisements. Unlike the original BU cost function model, a new method to determine λ_S and μ_D is proposed. To determine μ_D, we calculate the average time period between consecutive session arrivals t_a and the average session duration t_d, both of which must be continuously updated as soon as new values are generated each time a session arrives at the MN or a previous session ends. However, the recent events must influence t_a and t_d more than the earlier ones. When there are t events, we always have

$$t_a = (1 - \alpha)t_a(t - 1) + \alpha t_{aNew}, \tag{14}$$

$$t_d = (1 - \beta)t_d(t - 1) + \beta t_{dNew}. \tag{15}$$

Two weight parameters, α and $\beta (0 \leqslant \alpha, \beta \leqslant 1)$, have been introduced to assign recent events a heavier weight than the earlier ones. In our simulations, α and βwere set to $\frac{1}{4}$. The parameters t_{aNew} and t_{dNew} denote the recently generated values. Finally, we compare t_a with t_d and set the mean inter-session time to t_a if $t_a \geqslant t_d$. In case if $t_a < t_d$, the mean inter-session time is set to t_d. As the inter-session time is assumed to follow an exponential distribution with the parameter λ_S and expectation $\frac{1}{\lambda_S}$, λ_S is given by

$$\lambda_S = \begin{cases} \frac{1}{t_a}, & \text{if } t_a \geqslant t_d, \\ \frac{1}{t_d}, & \text{otherwise}, \end{cases} \tag{16}$$

Considering a high speed MN, it is most likely that it will spend less time in its MAP domain than a lower speed one. Therefore, μ_D is expressed with respect to the MN's speed. Initially, the domain size of a possible MAP candidate is determined. Fig. 2 shows an MN that has just left its domain and is now in the range of MAP Domains 1 and 2. The MN, moving in the direction indicated by the arrow, must now choose the most suitable MAP. Although MAP Domain 1 is larger than MAP Domain 2, the MN should obviously be bound to MAP 2, as it will soon go beyond MAP 2's domain range. This example makes it clear that considering only the range of an MAP domain without taking into account its direction of movement can not always guarantee the most appropriate MAP selection. Therefore, the domain size is calculated based on the probability that the MN actually enters subnets of the domain. For implementation, the AR should maintain information about (1) the locations

Please cite this article in press as: J. Baek et al., On a moving direction pattern based MAP selection model for HMIPv6 networks, Comput. Commun. (2010), doi:10.1016/j.comcom.2010.03.030

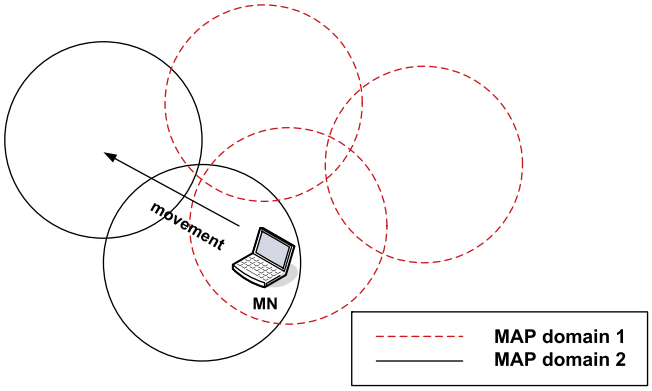

Fig. 2. Effect of MAP domain size.

of available MAPs; and (2) from where the MN entered its current network. Based on the locations of MAPs, the groups of MAPs are categorized by eight different directions. The first group is the set of MAPs, which are located in the same direction as the MN's current direction of movement. The other direction groups are at angles of 45° with respect to each other. Each direction group of MAPs is assigned a probability, indicating the likelihood that the MN actually moves in that direction. The actual size of an MAP domain is then calculated via

$$E(r_{MD}) = \sum_{d=1}^{8} \left\{ P(X = d) \sum_{j=1}^{n} X_{A_d}(s_j) \right\}, \tag{17}$$

where r_{MD} is the range of the MAP domain and X is a parameter. The parameter d has a value between one to eight, corresponding to the eight possible directions of movement of the MN, n refers to the number of subnets within the MAP domain, and s_j denotes the subnet j of the MAP domain. $X_{Ad}(s_j)$ describes the characteristic function of the set A_d. A_d contains all subnets of the MAP, which are crossed when the MN moves in direction d. Therefore, $X_{Ad}(s_j)$ is given by

$$X_{A_d}(s_j) = \begin{cases} 1, & \text{if } s_j \in A_d, \\ 0, & \text{otherwise}, \end{cases} \tag{18}$$

Using $E(r_{MD})$, we can obtain the number of MAP domain subnets that are actually used by the MN. Let t_{sub} be the average subnet residence time of an MN. To determine t_{sub}, we measure the time between two consecutive handoffs by subtracting the time that an MN enters a subnet from the time the MN leaves it. This procedure must be performed for every subnet handoff. As was the case for t_a and t_d, which are expressed by Eqs. (14) and (15), we assign a greater weight to recently calculated subnet residence time than earlier ones, by introducing the weight parameter γ ($0 \leqslant \gamma \leqslant 1$). Then, the computation of t_{sub} can be expressed by

$$t_{sub} = (1 - \gamma) t_{sub}(t - 1) + \gamma\ t_{subNew}. \tag{19}$$

The average MAP domain residence time is then given by $E(r_{MD})t_{sub}$. As the MAP domain residence time is assumed to follow an exponential distribution with its parameter μ_D and expectation $\frac{1}{\mu_D}$, μ_D is given by

$$\mu_D = \frac{1}{E(r_{MD})t_{sub}}. \tag{20}$$

By considering the MAP domain size actually used and the MN's subnet residence time, we now have a precise description of the MN's MAP domain residence time.

3.2.2. PD cost function model

As a second metric for evaluating an MAP candidate, the proposed MAP selection scheme adopts the PD cost function defined in [15] after some modifications. We must distinguish two different transmission paths from CN-to-MN. One path uses route optimization and the other routes packets through MN's HA. To calculate the delivery costs per session, we define δ ($0 \leqslant \delta \leqslant 1$) as the ratio of packets not using route optimization and L_S as the average session size. P_N and P_O denote the packet delivery cost in the case of the non-optimized and optimized paths, respectively. Then, the packet delivery costs C_{PD} are given by

$$C_{PD} = \delta L_S P_N + (1 - \delta) L_S P_O. \tag{21}$$

PD costs are determined by the sum of transmission and processing costs. Transmission costs are proportional to the hop distance of the transmission path. Processing costs arise mainly at the HA and MAP. They include binding cache lookup costs for determining whether the packet must be tunneled to an MN, and a routing cost to determine the next hop. In the case of an MAP, the more MNs an MAP is currently serving, the higher the processing costs will be. Based on these observations, each MAP quantifies its current load, $load_{MAP}$, as an input parameter. Hence, the processing costs θ_{MAP} at the MAP are expressed with respect to its current load by

$$\theta_{MAP} = k_2 + \frac{load_{MAP}}{k_3}. \tag{22}$$

Unlike the original PD cost function model, the processing cost of the MAP is given by MAP's preference value, which is sent to the MN through the MAP option in RA messages. As for an MAP that is not currently serving any MN, the some processing costs also arise, and thus the constant k_2 ($k_2 \geqslant 0$) is introduced. In addition, the current MAP load is divided by k_3 ($k_3 \geqslant 0$), which is the number of MNs an MAP can handle. Finally, P_N and P_O are calculated by

$$P_N = T \sum_{i=0}^{D_N - 1} k_i + \theta_{HA} + \theta_{MAP}, \tag{23}$$

$$P_O = T \sum_{i=0}^{D_O - 1} k_i + \theta_{MAP}, \tag{24}$$

where T is the unit transmission costs, and D_N and D_O are the hop distances of the non-optimized path and the path using route optimization, respectively. θ_{HA} and θ_{MAP} denote the processing costs of the HA and MAP, respectively. Unlike the original PD cost function model, it is assumed that the hop distance between MAP and MN has no effect on the packet delivery costs. For example, let us assume MN1 is bound to a low-level MAP1 with hop distance one, and MN2 is bound to a high-level MAP2 with hop distance two. All MAPs are arranged in a tree-like manner. Both MNs are bound to the same AR and communicate with the same CN. Then, the total hop distance of "MN1–MAP1–CN" is the same as the hop distance of "MN2–MAP2–CN". Therefore, PD costs are independent of the hop distance. We can then assume that D_N and D_O are fixed. In addition, we recognize that the transmission cost can not be constant since each hop has a different traffic load over time. In order to scale the transmission cost, we introduce another coefficient k_i ($k_i \geqslant 0$), which is dependent on the current traffic for each hop.

3.2.3. Total cost per session

From the results given in the previous subsections, the total costs per session are given by

$$C_T = C_{BU} + C_{PD}. \tag{25}$$

Hence, an MN bound to a low-level MAP incurs lower PD and higher BU costs than an MN bound to a high-level MAP. The more sessions in which an MN is involved and the heavier traffic is sent by the MN

Please cite this article in press as: J. Baek et al., On a moving direction pattern based MAP selection model for HMIPv6 networks, Comput. Commun. (2010), doi:10.1016/j.comcom.2010.03.030

through the network, the greater the value of C_{PD} is. On the other hand, the faster an MN moves between subnets, the greater the cost of C_{BU} will be. By applying Eq. (25) to all available MAPs, an MN can rate the candidates and choose the most suitable MAP accordingly.

3.3. MAP selection

Based on the MAP evaluation, the MN selects and is bound to the MAP with the lowest total BU and PD costs, as expressed by

$$MAP_{chosen} \in \{MAP_i | C_{Ti} = \min(C_{Tj} | j \in MAP_{available})\}. \quad (26)$$

3.4. MAP revision

After being bound to the most suitable MAP, the MN continues to collect RA messages periodically during predefined time periods. Once the MN detects that its MAP is absent or a new MAP is available, it proceeds to the initialization phase again.

4. Performance analysis

The performance of the proposed MAP selection scheme is evaluated by conducting comprehensive simulations via a simulator developed in a Java platform. We compared our scheme with three existing MAP selection methods including FMS, MHDS and AMS. The proposed advanced adaptive MAP selection scheme is abbreviated as AAMS.

4.1. Simulation environment

The simulation environment is illustrated in Fig. 3. Our simulation topology consists of 64 subnets and a three-layer MAP hierarchy between Level 0 and Level 2. A Level 0 MAP has a domain size of 16 subnets, a Level 1 MAP domain consists of four subnets, and a Level 2 MAP serves one subnet. The simulation model was developed based on the following assumptions.

1. Initially, all MNs are uniformly distributed among the 64 subnets.
2. Each MN can move in eight different directions, as described in Section 3.2.1.
3. A Gamma distribution describes the subnet residence time of an MN with its shape parameter α and scale parameter β, as expressed by

$$f(x) = \frac{x^{\alpha-1} e^{\frac{-x}{\beta}}}{\Gamma(\alpha)\beta^{\alpha}}. \quad (27)$$

4. The Gamma function $\Gamma(\alpha)$ is defined as

$$\Gamma(\alpha) = \int_0^{\infty} t^{\alpha-1} e^{-t} dt. \quad (28)$$

5. The simulation model defines three speed classes for MNs, namely low speed, medium speed, and high speed. The expectations of the subnet residence time for each speed class, from the lowest to the highest, are 600, 330 and 60 time units, respectively. Accordingly, their variances are defined as 6000, 3300 and 600, respectively.
6. Each MN can move to one of the eight adjacent subnets when moving to another subnet. The mobility model is based on the MN's associated speed class. Low speed MNs switch to one of the neighboring subnets with the same probability of $\frac{1}{8}$. Medium and high speed nodes use a Gamma distribution defined earlier to determine their next subnet.
7. A Poisson distribution with the mean λ describes the session arrival process, as expressed by

$$f(x) = \frac{\lambda^k}{k!} e^{-\lambda}. \quad (29)$$

8. The duration of a session is characterized by a Pareto distribution with its shape parameter k ($k > 0$) and scale parameter x_{min} ($x_{min} > 0$), as expressed by

$$f(x) = \begin{cases} \frac{k}{x_{min}} \left(\frac{x_{min}}{k}\right)^{k+1}, & \text{if } x \geqslant x_{min}, \\ 0, & \text{otherwise}, \end{cases} \quad (30)$$

9. In our simulations, we set x_{min} to 180 and k to 0.78, as proposed in [20].
10. The simulation continues for 10,000 iterations, each of which lasts for one second.

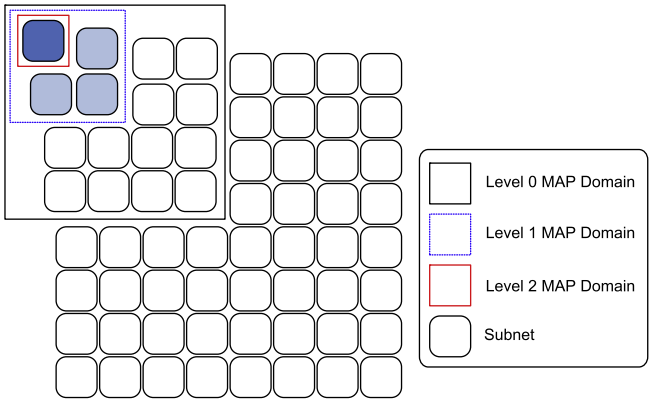

Fig. 3. MAP topology.

4.2. Simulation results

Three scenarios were established to test the efficiency of our proposed MAP selection scheme, each constructed with a distinct set of MNs as follows:

1. Scenario 0: 80% low speed, 20% medium speed, and 0% high speed MNs.
2. Scenario 1: 20% low speed, 60% medium speed, and 20% high speed MNs.
3. Scenario 2: 0% low speed, 20% medium speed, and 80% high speed MNs.

In the following subsections, all cost calculations are conducted for each scenario and all costs are expressed in terms of signaling traffic. In addition, we abbreviate the low-level, middle-level, and high-level MAPs as MAP2, MAP1 and MAP0, respectively. We also need to mention that there should be additional costs imposed by all four operational phases. However, we do not consider these costs here because (1) they are relatively constant compared to the communication cost; and (2) our interest is to show the relative performance improvement of the proposed scheme compared to the other schemes.

4.2.1. BU costs

In order to measure BU costs, we must differentiate two types of BUs: (1) BU-to-HA, and (2) BU-to-MAP. As an MN's HA is usually much further away than its MAP, BU-to-HA is much more expensive than BU-to-MAP. Furthermore, we must consider that the location of an available low-level MAP in the network hierarchy is closer to an MN than the location of a high-level MAP. Hence, it is cheaper to send a BU to a low-level MAP rather than a high-level MAP. BU costs are then calculated using the sum of BU-to-HA

Please cite this article in press as: J. Baek et al., On a moving direction pattern based MAP selection model for HMIPv6 networks, Comput. Commun. (2010), doi:10.1016/j.comcom.2010.03.030

and MAP, and multiplied by different weight values, derived from the previous discussions as follows:

$$BU = 10N_{HA} + 1N_{MAP2} + 2N_{MAP1} + 3N_{MAP0}, \quad (31)$$

where N_{HA}, N_{MAP2}, N_{MAP1}, and N_{MAP0} are the numbers of BU-to-HA and MAP, respectively, each assigned an appropriate weight based on their hop distance to the MN.

Fig. 4 shows the resulting BU costs depending on the MAP selection scheme and scenario used. The lowest BU costs are achieved by FMS. It is always bound to the MAP that is the furthest along the transmission route on HA-to-MN. Therefore, in our simulation environment, an MN using FMS always selects MAP0 as its most suitable MAP candidate. This results in the lowest number of BU-to-HA of all schemes. As BU-to-HA is the most expensive route, FMS outperforms all other schemes in terms of BU costs. However, we show that this scheme has drawbacks in terms of MAP load balance and PD costs. MHDS produces slightly higher BU costs than FMS, as it selects its most suitable MAP based on the speed of the MN. Hence, it is bound to MAP0 only if the MN has a high speed pattern. This costs more on BU-to-HA and therefore higher BU costs. AMS and AAMS select the MN's MAP based on an analytical cost function model. It considers not only BU costs but also PD costs and MAP load balance. This is the reason that BU costs alone seem to be significant. However, by treating total costs we show that these schemes outperform all the others.

4.2.2. PD costs

PD costs are calculated by monitoring the load of each MAP and the number of sessions that are handled by the MAP. We then calculate the processing overhead per session for every MAP based on its actual load using the second term of Eq. (22). The constant k_3 depends on the number of MNs an MAP can handle. In our simulations, k_3 is set to five and k_2 to one. Total processing costs are then calculated via Eqs. (23) and (24).

Furthermore, in order to distinguish packets per session that follow the route optimized path and packets per session that follow the non-optimized paths, we set δ to 0.05, θ_{HA} to one, L_S to 30, D_N to 20, and D_O to 10. PD costs were calculated for each new session that arrives at an MN through its MAP, based on the MAP's current load. Fig. 4 shows the resulting PD costs, depending on the MAP selection schemes and scenarios used.

FMS is the most expensive one in terms of PD costs. This is owing to the fact that all MNs are bound to MAP0, leading to a tremendous processing overhead. PD costs with MHDS are low for Scenario 0, as most of the MNs are low speed MNs and therefore are bound to low-level MAPs. Since there are 64 low-level MAPs, the load of a single MAP is sufficiently low. In the case of Scenario 2, however, most of the MNs are bound to high-level MAPs, but there are only four. This leads to a high processing overhead at these MAPs and incurs high PD costs. AMS has the explicit goal of minimizing total PD and BU costs. via its cost function model, it determines an appropriate MAP with the lowest PD and BU costs. AAMS definitely has the lowest PD costs in all scenarios, as it accommodates the cost function of AMS to include the current MAP load in its calculations.

4.2.3. Total costs

Total costs are then calculated by adding PD and BU costs. Fig. 4 shows the resultant total costs depending on the MAP selection schemes and scenarios considered. The greatest contribution to the total costs is PD costs, and hence FMS gives the highest total costs and MHDS the second highest, as they incur high PD costs. AMS shows low total costs, and however its costs are slightly higher than those of AAMS. Because of the great contribution of PD costs, AAMS can accommodate the highest BU cost and can still achieve the lowest total cost. AAMS outperforms all other schemes in every scenario. Although the total cost difference between the AMS and AAMS is not very significant at the MAP decision point, the resulting packet delivery delay becomes more prominent when an MN receives actual data packets from its CN because the small PD cost difference will repeatedly affect the data packet delivery delay in the session.

4.2.4. MAP load

To measure the balance of MAP selection, we determine the MAP load and calculate the variance from it. We examine two different MAP load schemes. The first scheme determines the MN distribution over three different MAP levels (i.e., low, middle, and

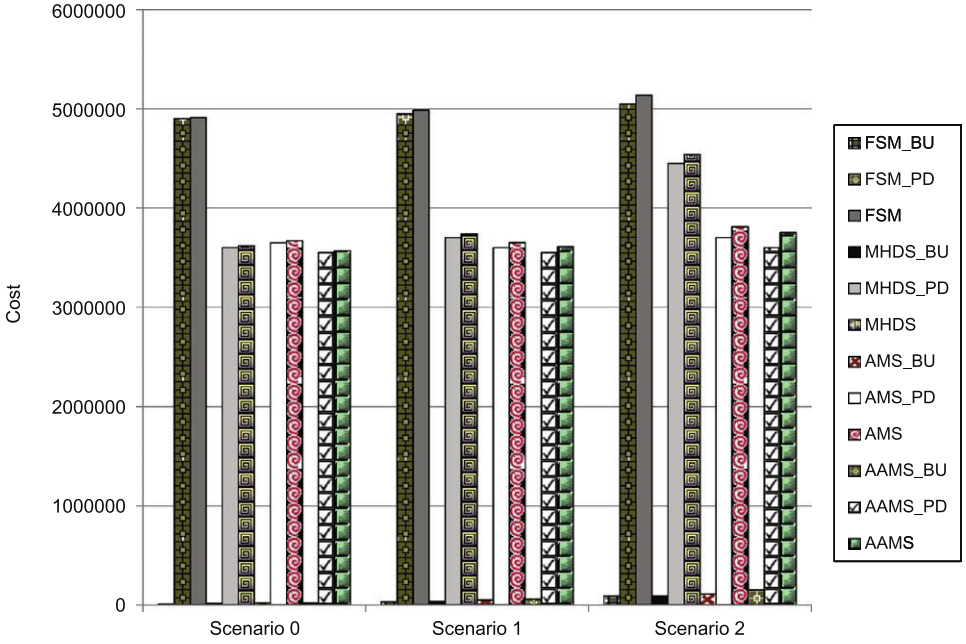

Fig. 4. BU, PD, and total costs.

Please cite this article in press as: J. Baek et al., On a moving direction pattern based MAP selection model for HMIPv6 networks, Comput. Commun. (2010), doi:10.1016/j.comcom.2010.03.030

high), without considering the number of MAPs at each level. For example, assume that there are 60, 30 and 10 MNs bound to low-level, middle-level, and high-level MAPs, respectively. Then, the MAP load distribution at MAP2, MAP1 and MAP0 is 60%, 30% and 10%, respectively. This scenario disregards the number of MAPs at each MAP level. However, it shows the general distribution of MNs among different MAP levels. Fig. 5 shows the simulation results in terms of the MAP load.

For FMS, all MNs always select MAP0 as their serving MAP, as shown in Fig. 5(a). A small percentage (< 1%) of MNs that are not bound to a high-level MAP is the result of the initial random distribution of MNs among MAPs. Therefore, FMS has the worst MAP load balance and hence the highest variance, as shown in Fig. 5(b).

As MHDS disregards the number of MAPs at each MAP level, the MAP load distribution is almost a precise copy of the speed class scenario that has been selected. This is a major drawback, as in the case of Scenario 2, MHDS binds 80% of MNs to a high-level MAP. Unfortunately, most network infrastructures have far fewer high-level MAPs than low-level MAPs, which eventually results in a bottleneck at these MAPs. AMS has high variance values for Scenarios 0 and 1. This is not bad at all, as AMS binds most MNs to low-level MAPs and there are a large number of low-level MAPs, and therefore the relative MAP load for each low-level MAP is sufficiently low. However, this is not true in the case of Scenario 2. It is clear that AAMS creates the most balanced MAP load among the three MAP levels.

The second metric also considers different numbers of MAPs at each MAP level. In order to deal with the example of the first MAP load scheme, let us consider 64, 16 and 4 low-level, middle-level and high-level MAPs, respectively. Hence, on the average there are $\frac{60}{64} = 0.93$ MNs bound to a low-level MAP, $\frac{30}{16} = 1.875$ MNs bound to a middle-level MAP, and $\frac{10}{4} = 2.5$ MNs bound to a high-le-

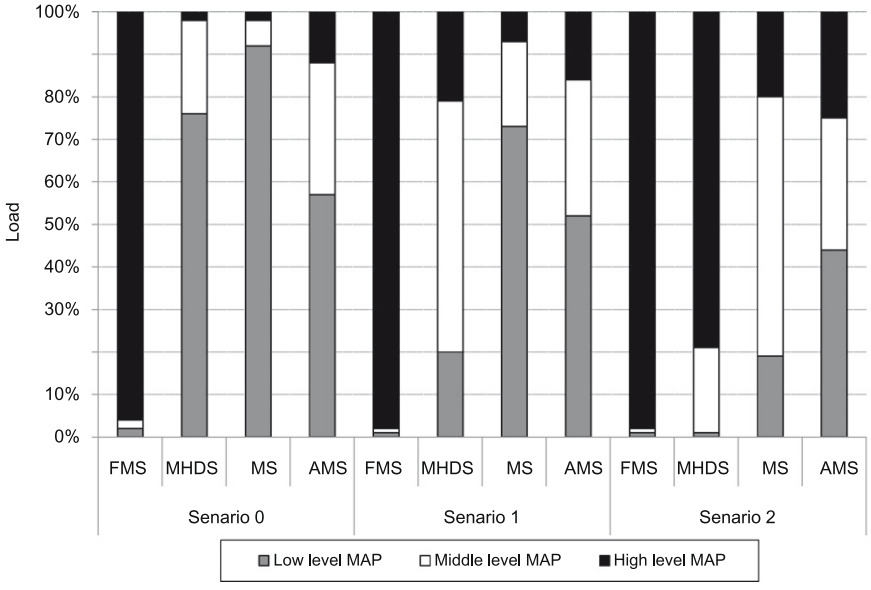

(a) MAP load with different schemes.

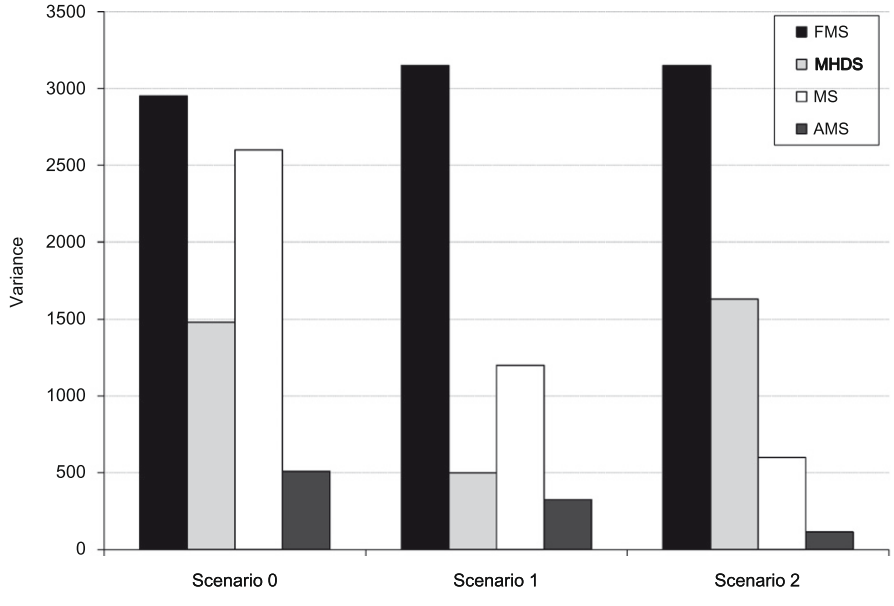

(b) Variance of MAP load.

Fig. 5. MAP load correlated with the MAP hierarchy level, disregarding the number of MNs at each level.

Please cite this article in press as: J. Baek et al., On a moving direction pattern based MAP selection model for HMIPv6 networks, Comput. Commun. (2010), doi:10.1016/j.comcom.2010.03.030

vel MAP. This results in a completely different MAP load distribution from that of the first MAP load scheme, as it needs to compare the utilization of a single MAP at one level with a single MAP at another level. Here, the result is 18%, 36% and 46% for low-level, middle-level, and high-level MAPs, respectively. Fig. 6 shows the simulation results.

As for the first MAP load scheme, FMS shows the worst load balance. MHDS achieves a good variance for Scenario 0 because of the beneficial speed class distribution in this scenario. As this scenario consists of 80% low speed nodes, MHDS binds approximately 80% of all MNs to low-level MAPs, and there are a large number of these in our simulations. The relative MAP load, which is correlated with the number of MAPs at each MAP level, is therefore quite low. AMS and AAMS can maintain a constantly low variance value in all scenarios. However, AAMS attains a better MAP balance in an environment with a large number of low speed MNs.

5. Conclusions and future works

HMIPv6 was introduced to reduce the signaling overhead during the handoff procedure by establishing MAPs. We proposed a novel MAP selection scheme to support HMIPv6 in a multi-MAP environment. Our proposed MAP selection scheme uses a cost function model that enables an MN to rank all available MAPs and bind to the most appropriate one. We considered all important factors that influence the MAP selection process, including MN speed and direction of movement, MAP load, and BU and PD costs. Simulation results showed that our scheme outperforms FMS, MHDS and AMS in terms of total PD and BU costs. Compared to AMS, our scheme achieves a similar MAP load balance. AAMS performs well in terms of signaling traffic and MAP load balance. However, it has some limitations. The computational overhead of AAMS is slightly higher than that of AMS. We believe this overhead

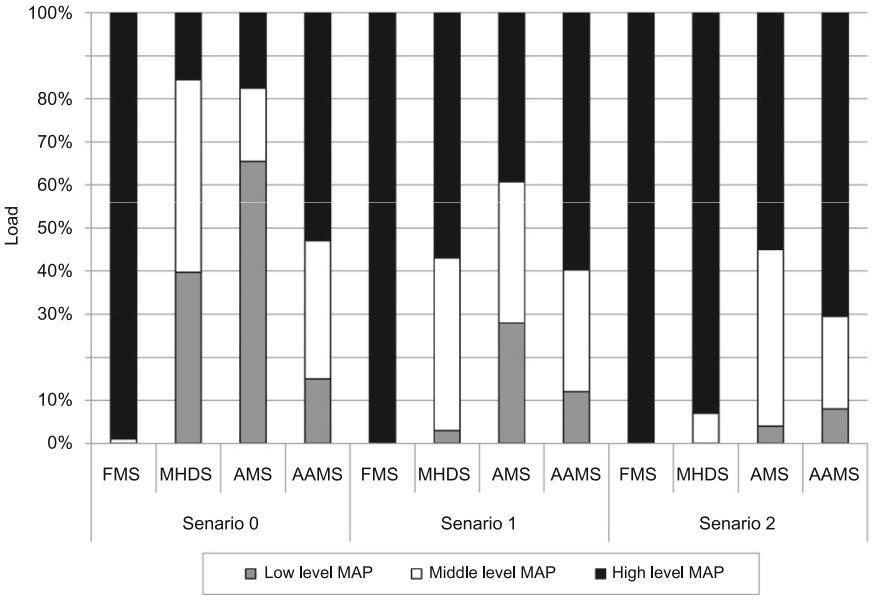

(a) MAP load with different schemes.

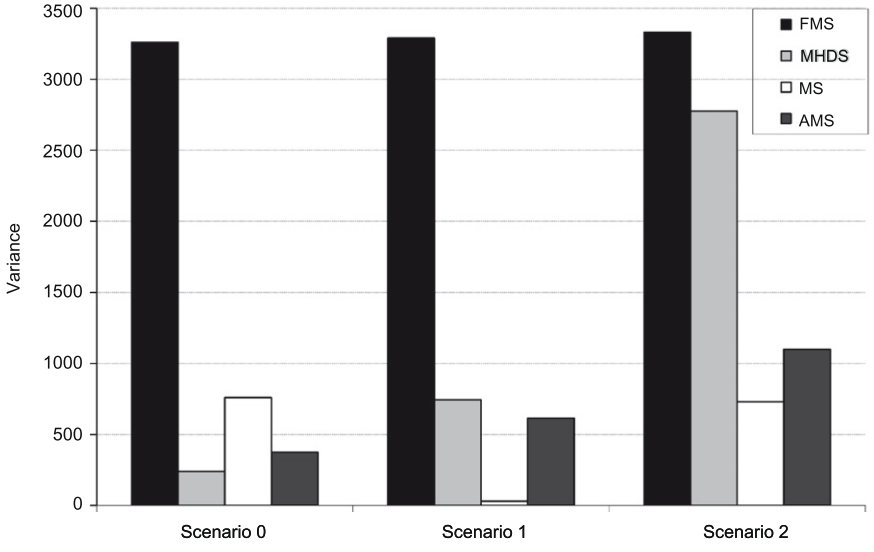

(b) Variance of MAP load.

Fig. 6. MAP load correlated with the MAP hierarchy level, considering the number of MNs at each level.

Please cite this article in press as: J. Baek et al., On a moving direction pattern based MAP selection model for HMIPv6 networks, Comput. Commun. (2010), doi:10.1016/j.comcom.2010.03.030

can be reduced sufficiently by allowing an MN to select the MAP having the least cost. Also, handover delay due to the computation overhead can be leveraged by some mobility prediction algorithms. Subsequently, MAP selection can be performed even before an MN actually moves into a different domain. In order to apply our scheme to real mobile networks, the comprehensive implementation of HMIPv6 should precede the proposed scheme. As it intends to reduce signaling requirements outside the access network where the service is provided, mobility management modules should first be developed. In addition, the implementation should include modules to support (1) functional MAP hierarchy for all available MAPs, (2) dynamic MAP propagation using RA messages, and (3) all IPv6 transport layers, alternative CoA, and RCoA. Given this framework, we can develop an additional module to reduce BU and PD costs for an MN. We plan to do some more works on the handover delay in the future as well.

Acknowledgement

This research was supported by Ministry of Culture, Sports and Tourism (MCST) and Korea Culture Content Agency (KOCCA) in the Culture Technology (CT) Research & Development Program, the Korean government. This research was supported by the Brain Korea 21 program, Ministry of Education, Science and Technology, the Korean government and Taiwan National Science Council research Grant NSC98-2219-E-006-011.

References

[1] E. Lee, J. Baek, S. Huang, A dynamic mobility management scheme for VoIP services, in: Proceedings of IEEE ITNG, April 2006, pp. 340–345.
[2] E. Gustafsson, A. Jonsson, C. Perkins, Mobile IP regional registration, IETF RFC 2002, March 2001.
[3] C. Perkins, IP mobility support, IETF RFC 2002, 1996.
[4] C. Perkins, Route optimization in mobile IP, IETF Draft, draft-ietf-mobileip-08.txt, September 2001.
[5] D. Johnson, J. Arkko, Mobility support in IPv6, IETF RFC 3775, June 2004.
[6] H. Soliman, C. Castelluccia, K. El Malki, L. Bellier, Hierarchical mobile IPv6 mobility management (HMIPv6), IETF RFC 4140, August 2005.
[7] J. Baek, P.S. Fisher, M. Kwak, FI-based local group key generation/distribution for mobile multicast in a hierarchical mobile IPv6 network, KSII Transactions on Internet and Information Systems 2 (1) (2008) 5–22. February.
[8] M. Kim, H. Radha, J.Y. Lee, H. Choo, An efficient multicast-based binding update scheme for network mobility, KSII Transactions on Internet and Information Systems 2 (1) (2008) 23–36. February.
[9] H.Q. Vo, D. Kim, C.S. Hong, S. Lee, E-N. Huh, A novel scheme for seamless handoff in WMNs, KSII Transactions on Internet and Information Systems 3 (4) (2009) 399–422. August.
[10] B. Park, E. Hwang, G-C. Park, Seamless mobility management in IP-based wireless/mobile networks with fast handover, KSII Transactions on Internet and Information Systems 3 (3) (2009) 266–285. June.
[11] W. Chung, S. Lee, Cost-effective MAP selection in HMIPv6 networks, in: Proceedings of IEEE ICC, June 2007, pp. 6026–6031.
[12] W. Chung, S. Lee, Improving performance of HMIPv6 networks with adaptive MAP selection scheme, IEICE Transactions on Communications E90-B (4) (2007) 769–776. April.
[13] K. Kawano, K. Kinoshita, K. Murakami, A multilevel hierarchical distributed IP mobility management scheme for wide area networks, in: Proceedings of IEEE ICCCN, October 2002, pp. 480–483.
[14] W. Ma, Y. Fang, Dynamic hierarchical mobility management strategy for mobile IP networks, IEEE Journal on Selected Areas in Communications 22 (4) (2004) 664–676. May.
[15] S. Pack, M. Nam, T. Kwon, Y. Choi, An adaptive mobility anchor point selection scheme in hierarchical mobile IPv6 networks, Elsevier Computer Communications (2005) 3066–3078. June.
[16] V.L.L. Thing, H.C.J. Lee, Y. Xu, A local mobility agent selection algorithm for mobile networks, in: Proceedings of IEEE ICC, May 2002, pp. 465–469.
[17] V.L.L. Thing, H.C.J. Lee, Y. Xu, History-based auxiliary mobility management strategy for hierarchical mobile IPv6 networks, IEICE Transactions on Fundamentals of Electronics, Communications, and Computer Science E88-A (7) (2005) 1845–1858. July.
[18] Y.-H. Wang, K.-F. Huang, C-S. Kuo, W-J. Huang, Dynamic MAP selection mechanism for HMIPv6, in: Proceedings of ICAINA, March 2008, pp. 691–696.
[19] Y. Xu, H.C.J. Lee, V.L.L. Thing, A local mobility agent selection algorithm for mobile networks, in: Proceedings of IEEE ICC, May 2003, pp. 1074–1079.
[20] A. Balachandran, G.M. Voelker, P. Bahl, P.V. Rangan, Characterizing user behavior and network performance in a public wireless LAN, ACM SIGMETRICS Performance Evaluation Review 30 (1) (2002) 195–205. June.

Please cite this article in press as: J. Baek et al., On a moving direction pattern based MAP selection model for HMIPv6 networks, Comput. Commun. (2010), doi:10.1016/j.comcom.2010.03.030